# Simulations of Gas Cloud Expansion Using A Multi-Temperature Gas Dynamics Model

Virendra K. Dogra, Jeff C. Taylor
Robert E. Erlandson and P. K. Swaminathan
*The Johns Hopkins University Applied Physics Laboratory*
*Laurel, Maryland 20723, USA*

Robert P. Nance
*Naval Surface Warfare Center*
*Dahlgren, Virginia 22448, USA*

**Abstract.** Simulations are performed using a multiple temperature gas model to investigate translational non-equilibrium effects in a rapid expansion of a high temperature argon gas cloud into a rarefied atmosphere. A set of continuum conservation equations based on kinetic theory, which includes anisotropic forms for the temperature, pressure and speed ratio, are solved numerically using a flux splitting scheme for the inviscid fluxes and a central difference scheme for the viscous fluxes in a time accurate manner. Results obtained for the initial expansion of the spherical gas cloud from a high density source condition show that translational non-equilibrium exists in the shock front region which propagates into the ambient atmosphere. For a lower density source condition, translational non-equilibrium not only exists in the shock front but also in the inner gas cloud region where the temperature normal to the radial direction freezes at a value just below the initial source temperature.

## Introduction

The expansion of a high temperature gas cloud in a rarefied environment is a phenomenon that has many applications in space from supernova explosions to recent active space experiments[1] where the interaction of an artificial plasma gas cloud with the ambient atmosphere was studied. In the rapid expansion of a gas cloud, a spherical shock wave front propagates into the ambient atmosphere followed by a contact surface, which separates the expanding gas cloud mass from that of the ambient environment, and a rarefaction wave propagates towards the center of the source in the expanding gas. Recent time-accurate continuum simulations[2,3] of a high temperature metallic gas cloud at high altitude with radiation transport show that extremely high velocities along with material phase change can occur in the flow of such a gas cloud expansion. Calculated values[2,3] of the continuum break down parameter proposed by Bird suggest that in some parts of the flow, especially in the shock region, the non-equilibrium effects dominate the flow structure. Thus, it appears that particle simulation methods such as the direct simulation Monte Carlo (DSMC) method[4] would be more suitable for simulating these flows. However, the presence of radiation and unsteady behavior in these flows makes the particle simulations a formidable computational task. Moreover, the high densities in the source region along with the phase changes encountered in the flow present further problems with the dilute gas assumptions made in these particle simulation methods. Experimental investigation of the initial evolution of such a gas cloud is also complicated by the very small time scales involved and optical opaqueness near the gas source. This suggests that, at present, a continuum method which to some extent accounts for non-equilibrium effects in the flow will be optimum in predicting the early expansion of such a high temperature gas cloud.

In the present study the time accurate numerical simulations of a rapidly expanding high temperature argon gas cloud are performed using continuum conservation equations with

# REPORT DOCUMENTATION PAGE

Form Approved OMB No. 0704-0188



| 1. REPORT DATE (DD-MM-YYYY) | 2. REPORT TYPE | 3. DATES COVERED (FROM - TO) |
|---|---|---|
| 09-07-2000 | Conference Proceedings | 09-07-2000 to 14-07-2000 |

4. TITLE AND SUBTITLE
Simulations of Gas Cloud Expansion Using A Multi-Temperature Gas Dynamics Model
Unclassified

5a. CONTRACT NUMBER
5b. GRANT NUMBER
5c. PROGRAM ELEMENT NUMBER

6. AUTHOR(S)
Dogra, Virendra K. ;
Taylor, Jeff C. ;
Erlandson, Robert E. ;
Swaminathan, P. K. ;
Nance, Robert P. ;

5d. PROJECT NUMBER
5e. TASK NUMBER
5f. WORK UNIT NUMBER

7. PERFORMING ORGANIZATION NAME AND ADDRESS
The Johns Hopkins University Applied Physics Laboratory
Laurel, MD20723

8. PERFORMING ORGANIZATION REPORT NUMBER

9. SPONSORING/MONITORING AGENCY NAME AND ADDRESS
AOARD
Unit 45002
APO AP, xx96337-5002

10. SPONSOR/MONITOR'S ACRONYM(S)
11. SPONSOR/MONITOR'S REPORT NUMBER(S)

12. DISTRIBUTION/AVAILABILITY STATEMENT
APUBLIC RELEASE
,

13. SUPPLEMENTARY NOTES
See Also ADM001341, Rarefied Gas Dynamics (RGD) 22nd International Symposium held in Sydney, Australia, 9-14 July 2000.

14. ABSTRACT
Simulations are performed using a multiple temperature gas model to investigate translational non-equilibrium effects in a rapid expansion of a high temperature argon gas cloud into a rarefied atmosphere. A set of continuum conservation equations based on kinetic theory, which includes anisotropic forms for the temperature, pressure and speed ratio, are solved numerically using a flux splitting scheme for the inviscid fluxes and a central difference scheme for the viscous fluxes in a time accurate manner. Results obtained for the initial expansion of the spherical gas cloud from a high density source condition show that translational non-equilibrium exists in the shock front region which propagates into the ambient atmosphere. For a lower density source condition, translational non-equilibrium not only exists in the shock front but also in the inner gas cloud region where the temperature normal to the radial direction freezes at a value just below the initial source temperature.

15. SUBJECT TERMS

| 16. SECURITY CLASSIFICATION OF: | | | 17. LIMITATION OF ABSTRACT | 18. NUMBER OF PAGES | 19. NAME OF RESPONSIBLE PERSON |
|---|---|---|---|---|---|
| a. REPORT | b. ABSTRACT | c. THIS PAGE | Public Release | 8 | Fenster, Lynn<br>lfenster@dtic.mil |
| Unclassified | Unclassified | Unclassified | | | 19b. TELEPHONE NUMBER<br>International Area Code<br>Area Code Telephone Number<br>703767-9007<br>DSN<br>427-9007 |

anisotropic temperature gas models[5-7] This model accounts for translational non-equilibrium effects and is appropriate for these simulations. The equations are solved numerically using the kinetic flux splitting method[8] for the inviscid fluxes and central difference scheme for the dissipative fluxes. The purpose of this study is to provide fundamental understanding of the initial evolution of a rapidly expanding gas cloud and propagation of the associated shock front in the ambient atmosphere where translational non-equilibrium effects become important. Results using Navier-Stokes calculations for the dense source condition are presented for comparison.

## Gas Dynamics Model

The flow is governed by one-dimensional/spherically symmetric conservation equations of gas dynamics, modified to account for translational non-equilibrium. These modified equations are derived from a first-order Chapman-Enskog expansion of the Boltzmann equation using an anisotropic distribution function. This approach is quite similar to that followed by Candler, Nijhawan *et al*.in their investigation of the normal shock structure[7]. In integral-vector form, the equations can be written as

$$\frac{\partial}{\partial t}\int_V Q\,dV + \oiint_S F_Q \cdot dS = S$$

where the conserved quantities per unit volume are given by

$$Q = \begin{bmatrix} \rho \\ \rho v_r \\ \rho e_{tr} \\ \rho e_{tp} \end{bmatrix} .$$

Only one of the two components of the translational specific energy that is perpendicular to the radial direction ($e_{tp}$) is considered because the two perpendicular components are equal. The gas dynamics flux vectors are given by

$$F_Q = \begin{bmatrix} \rho v_r \\ \rho v_r^2 + p_r + radial\ componets\ of\ p_p\ and\ p_t \\ \langle \rho e_{tr} + p_r \rangle v_r + q_{rr} \\ \rho e_{tp} v_r + q_{pr} \end{bmatrix}$$

and the source terms are

$$S = \begin{bmatrix} 0 \\ 0 \\ S_r \\ S_p \end{bmatrix}$$

with

$$e_{tr} = \frac{1}{2} R T_r + \frac{1}{2} v_r^2 \qquad \text{(total specific energy in radial direction)}$$

$$e_{tp} = \frac{1}{2} R T_p \qquad \text{(total specific energy in one perpendicular direction)}$$

$$q_{rr} = - k_{rr} \frac{\partial T_r}{\partial r} \quad , \qquad \text{where} \quad k_{rr} = \frac{3}{2} \frac{m_{ref}}{T_{ref}} R T_r$$

$$q_{pr} = - k_{pr} \frac{\partial T_p}{\partial r} \quad , \qquad \text{where} \quad k_{pr} = \frac{1}{3} k_{rr}$$

$$p_r = \rho R T_r \quad , \qquad p_p = \rho R T_p \quad .$$

The source terms considered in the present formulation are assumed to be for Maxwell molecules gas. Thus, the source terms are as (Ref.7)

$$S_r = \frac{1}{3} \rho R \frac{T_{ref}}{m_{ref}} \langle p_p - p_r \rangle \quad , \qquad S_p = -\frac{1}{2} S_r$$

where $\rho$ is the mass density, $v_r$ is the radial velocity, $T_r$ is the gas temperature in radial direction, $T_p$ is the temperature in one perpendicular direction and $R$ is the gas constant. The expression for $k_{rr}$ and $k_{pr}$ above are for Maxwell molecules.

## Computational Approach

The gas dynamic equations listed above are solved numerically in a time accurate manner. The inviscid part of the flux, $F_Q$, is calculated at each cell interface using a kinetic flux splitting method.[8] A local ellipsoidal distribution function of the form

$$f_0 = f_{0r} \, f_{0p} \, f_{0t}$$

where

$$f_{0r} = \frac{1}{\sqrt{2 \pi R T_r}} \exp\langle - \frac{1}{2 R T_r} c_r'^{\,2} \rangle,$$

$$f_{0p} = \frac{1}{\sqrt{2 \pi R T_p}} \exp\langle - \frac{1}{2 R T_p} c_p'^{\,2} \rangle,$$

$$f_{0t} = \frac{1}{\sqrt{2 \pi R T_t}} \exp\langle - \frac{1}{2 R T_t} c_t'^{\,2} \rangle,$$

is then defined for each cell and used to formulate analytical expressions for the inviscid fluxes in both the radial and perpendicular directions. The $c'_r$, $c'_p$, and $c'_t$ are the components of the random molecular velocity in the above expressions. As with other flux-splitting techniques, this inviscid flux is formally first-order accurate in space. Second-order accuracy in space is achieved by using a MUSCL variable-extrapolation scheme[9] in conjunction with a minmod slope limiter to ensure monotonicity Viscous fluxes are calculated with a second-order accurate central difference scheme.

Fourth-order accuracy in time is obtained using a Runge-Kutta time integration method[10]. The time step is chosen as the minimum of a Courant-based time step and a step based on the magnitude of energy exchange between radial and perpendicular directions.

## Results and Discussion

The high temperature argon gas cloud assuming the interatomic potential to be Maxellian (inverse fourth power) ($T_{ref} = 273\,K$ *and* $m_{ref} = 2.517\,x\,10^{-5}\ kg/m\,s$) is initialized as a sphere of radius 0.03 m with a uniform density and temperature. The initial density and temperature of the gas cloud are assumed to be 20 kg/m$^3$ and 10,000 K, respectively. The argon cloud in equilibrium at this temperature would be partially ionized, but its thermal energy would still be much larger than the electromagnetic potential energy. Thus, the electromagnetic effects can be neglected for the initial evolution of the gas cloud expansion.

The initial spherical volume is divided into 240 uniformly distributed cells. One cell is added to the outer boundary after each time step allowing grid to grow in time as the gas cloud expands. The procedure reduces the computational task during early phases of the solution because computation may need up to 100,000 cells at later times. The outer boundary condition is assumed to be the undisturbed ambient conditions. The ambient conditions for this study correspond to 60 km altitude. Thus, the density and temperature used are 3.09 x $10^{-4}$ kg/m$^3$ and 247 K, respectively. To focus on the cloud expansion and not on molecular diffusion and other multi-species issues, the ambient atmosphere is simulated as pure argon at the ambient atmospheric density and temperature.

Figures 1-4 show the flow structure of the spherical gas cloud expansion at three different times. These figures show that a well-defined shock wave propagates outward in the ambient atmosphere. The shock is followed by a contact surface, which separates the expanding gas from the ambient environment. A strong rarefaction wave travels behind the contact surface towards the center of the source. Figures 1-3 also show that density, temperature and pressure decrease in the source region as time increases. The magnitude of the density ratio across the shock remains almost the same as the gas expands (Fig. 1). However, the temperature and pressure ratios across the shock decrease gradually as the gas cloud expands (Figs. 2-3).

Figure 2 shows that the minimum radial and perpendicular temperatures in the gas cloud behind shock front can fall significantly lower than the ambient temperature. This is due to the strong rarefaction wave that propagates in the opposite direction of the shock wave. Similarly, the radial and perpendicular components of the pressure behind the shock front fall lower than the ambient pressure value with time as gas expands (Fig. 3).

In Fig. 4 the radial velocity profiles are shown as a function of normalized radial distance at different times. The radial velocity increases linearly through the cloud with increasing radius for most of the flowfield. Also, the radial velocity gradient decreases with time as the gas cloud expands. The peak velocities predicted for the first 1.2 x $10^{-4}$ s in the gas cloud expansion are more than 3 km/s (Fig. 4).

Translational non-equilibrium is evident in the shock wave as the gas cloud expands (Figs. 5-6). Figure 2 and Figs. 5-6 show that the most of the inner part of the gas cloud remains in translational equilibrium. This results because the mass density is still high enough in the cloud to equilibrate the translational modes at this initial phase of the gas expansion. There is an observed overshoot in the radial temperature just behind the shock wave, but no overshoot is observed in the perpendicular temperature at these conditions (Fig.2).

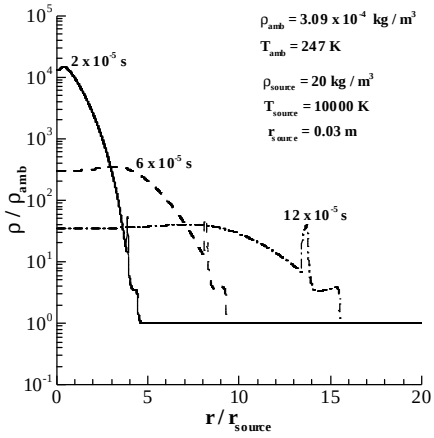


**Fig 1**: Density Profiles

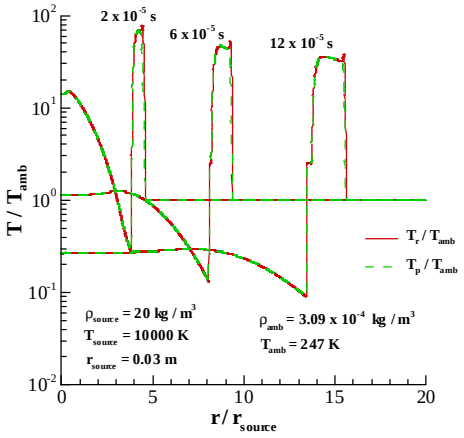


**Fig 2**: Temperature Profiles

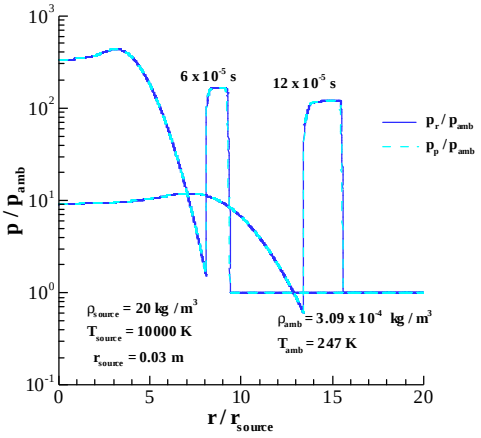


**Fig 3**: Pressure Profiles

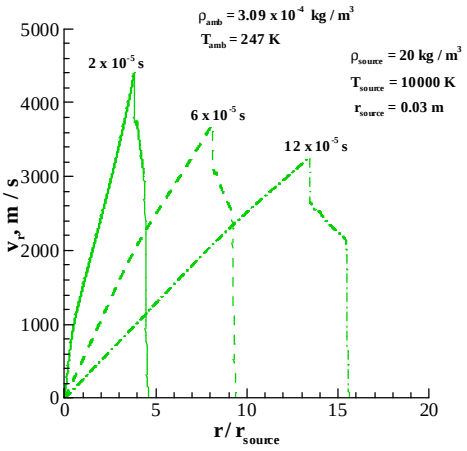


**Fig 4**: Radial Velocity Profiles

Figures 5-8 show the detailed shock wave front structure. The radial and perpendicular temperatures profiles near the shock wave for two different times (4 x $10^{-5}$ s and 12 x $10^{-5}$ s) are shown in Figs. 5-6. It can be seen from these figures that thermal non-equilibrium exists just behind the shock where the radial and perpendicular temperature differ. The radial temperature overshoot increases with time as is demonstrated in Figs. 5-6 where the overshoot in radial temperature at 2 x $10^{-5}$ s is about 12% whereas at 12 x $10^{-5}$ s the overshoot is about 19%. Although the ratio of the overshoot to the equilbrium value increases with time, the magnitude of the overshoot radial temperature decreases with time. The translational non-equilibrium in the shock wave region can also be seen in pressure profiles (Figs. 7-8), where, the perpendicular pressure in the shock wave region lags behind the radial pressure. There is no overshoot in radial or perpendicular pressure profiles like those observed in the radial temperature profiles.

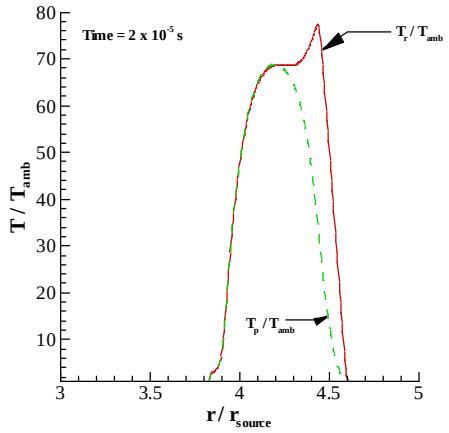


**Fig 5**: Shock Front Temperature Profiles

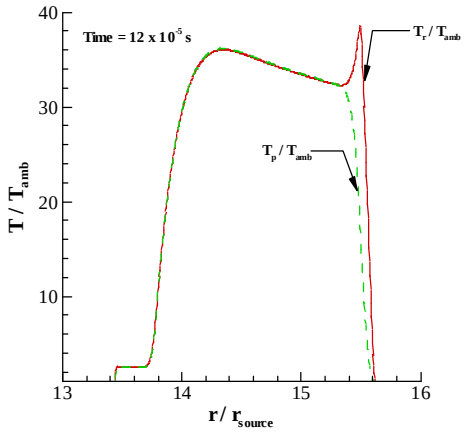


**Fig 6**: Shock Front Temperature Profiles

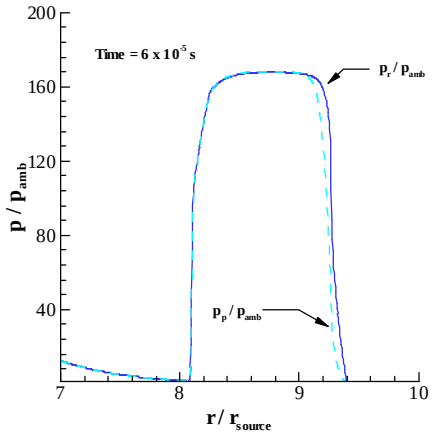


**Fig 7**: Shock Front Pressure Profiles

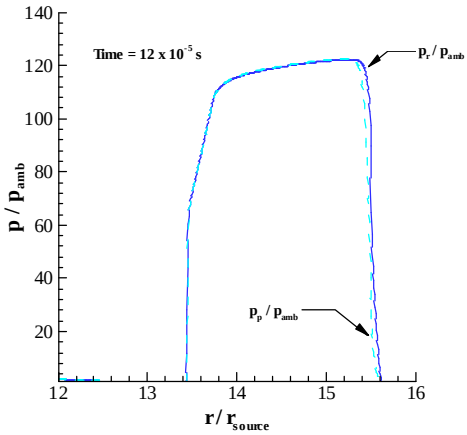


**Fig 8**: Shock Front Pressure Profiles

Figure 9 shows that the shock front location from the Navier-Stokes calculations leads the shock front location from the multi-temperature model calculations. This is probably due to differences in the calculation of the thermal radial momentum flux. For the multi-temperature model, the thermal radial momentum flux is equal to radial pressure, whereas, for the Navier-Stokes equations it is the sum of the isotropic pressure and the viscous stress in the radial direction, which depends on the radial velocity gradient. In the dense region of the source the density profiles from both methods compare well (Fig. 9).

A second set of calculations is also performed for a rarefied source condition. The radius of the initial source considered for this set of calculations is 0.05 m and the source density and temperature are 100 times higher than the ambient values. The ambient values of density and temperature are 7.971 x $10^{-7}$ kg/$m^3$ and 194.3 K, respectively. These correspond to an altitude of approximately 100 km. Figure 10 shows the normalized plots of density, radial temperature, and normal temperature as a function of the normalized radial distance. Strong translational non-equilibrium is observed well into the source region where the perpendicular temperature is frozen at a value slightly lower than the source value, whereas the radial temperature decreases rapidly

with the expansion of the gas cloud. The perpendicular temperature lags behind the rise in the radial temperature in the shock front. However, in the source region, the radial temperature is lower than the perpendicular temperature due to the large rarefaction effects at these conditions. Thus, significant thermal non-equilibrium can also be observed in the source region in the initial phase of the expansion if the initial density of the source is sufficiently low.

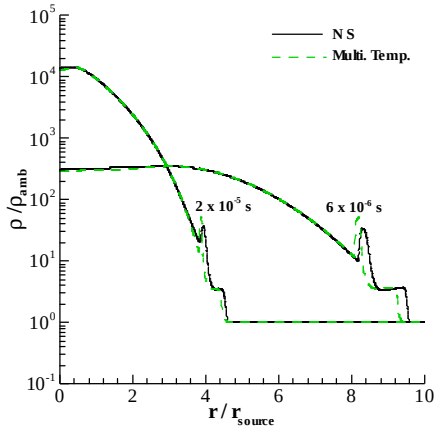


**Fig 9**: Density Profiles Comparison

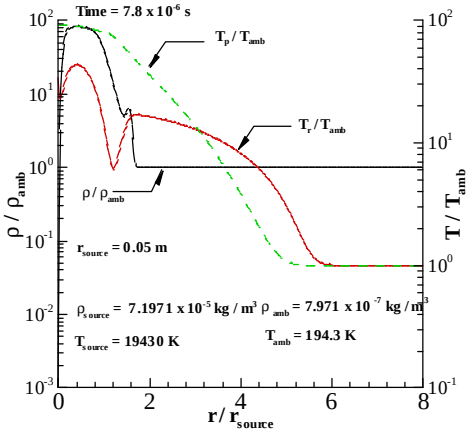


**Fig 10**: Density and Temperature Profiles

## Conclusions

A kinetic theory based flux vector splitting scheme has been successfully employed for the calculations of the inviscid fluxes of the continuum model with translational non-equilibrium. This approach allows the analytical formulation of the inviscid fluxes of the conserved quantities in the different characteristic directions.

Computations carried out for two distinct source conditions indicate that the shock wave front that propagates through an ambient atmosphere will exhibit translational non-equilibrium for all the source conditions considered. For the less dense source condition, the translational non-equilibrium not only exists in the region of the shock front but throughout most of the gas cloud expansion. The multi-temperature model predicts a radial temperature overshoot in the shock front for the dense source conditions and this radial temperature overshoot to the equilibrium temperature in the shock increases as the gas cloud expands. Comparison of the multi-temperature model results with the Navier-Stokes calculations shows that the shock front location in the Navier-Stokes calculations leads that predicted by the multi-temperature model because the Navier-Stokes equations do not have the translational non-equilibrium included in the formulation of the momentum flux. However, in the other regions of the gas cloud expansion where flow exhibits translational equilibrium, the two methods give similar results.

## References


1. Erlandson, R. E., Swaminathan, P. K., Meng, C.-I., Stoyanov, B. J., Zetzer, J. I., Gavrilov, B. G., Kiselev, Yu. N., and Romanovsky, Yu. A., "Observation of Auroral Emissions Induced by Artificial Plasma Jets," *Geophysical Research Letters*, Vol. 26, No. 11, 1999, pp. 1553-1556.
2. Dogra, V. K., Nance, R. P., Taylor, J. C., Swaminathan, P. K., Erlandson, R. E., and Meng, C.-I., "Time–Dependent Modeling of Gas Cloud Expansion in the Ionosphere with Radiation Transport and Gas Dynamics Coupling," AIAA Paper 99-3561, 1999.

3. Dogra, V. K., Nance, R. P., Taylor, J. C., Swaminathan, P. K., Erlandson, R. E., and Meng, C.-I., "Modeling of Gas Cloud Expansion at High altitude with Radiation Transport," *Journal of Thermophysics and Heat Transfer*, Vol. 14, No. 3, July-September 2000.
4. Bird, G.A., Molecular Gas Dynamics and the Direct Simulation of Gas Flows, Clarendon Press, Oxford, England, 1994.
5. Hamel, B. B., and Willis, D. B., "Kinetic Theory of Source Flow Expansion with Application to the Free Jet," *Physics of Fluids*, 9, 829, 1966.
6. Edwards, R. H., and Cheng, H .K., " Steady Expansion of a Gas into a Vacuum," *AIAA Journal*, 4, 558, 1966.
7. Candler, G. V., Nijhawan, S., Bose Deepak, and Boyd, I.D., "A Multiple Translational Temperature Gas Dynamics Model," *Physics of Fluids*, Vol. 6, No. 11, 1994.
8. Pullin, D.I., "Direct Simulation for Compressible Inviscid Ideal-Gas Flow," *Journal of Computational Physics*, 34, pp. 231-244, 1980.
9. Van Leer, B., " Towards the Ultimate Conservative Difference Scheme. A Second Order Sequel to Godunov's method," *Journal of Computational Physics*, Vol. 32, 1979, pp. 263-275
10. Jameson, A., Schmidt, W., and Turkel, E., "Numerical Simulations of the Euler Equations by Finite Volume Methods using Runge-Kutta Time Stepping Schemes," AIAA Paper 81-1259, 1981.